JETIR.ORG ISSN: 2349-5162 | ESTD Year : 2014 | Monthly Issue
JOURNAL OF EMERGING TECHNOLOGIES AND INNOVATIVE RESEARCH (JETIR)
An International Scholarly Open Access, Peer-reviewed, Refereed Journal

Simulation of the Indirect Evaporative Cooling System using the 2-D Model Cross-flow for Cambodia's Climate Conditions

[1]Sophal Pey, [2]Sarin Chan, [3]Kinnaleth Vongchanh, [4]Pheakdey Choun

[1,4]ETM Master Student, [2]Assistance Professor, [3]Lecturer Researcher, and Head of Thermal Laboratory
[1]Department of Industrial and Mechanical Engineering,
[1]Institute of Technology of Cambodia, Phnom Penh, Cambodia

Abstract: The evaporative cooling (EC) system is regarded as an alternative air-cooling technique to the traditional vapor-compression systems, with reduced energy consumption and low carbon potential, and it is appropriate for a variety of air conditioning applications such as industrial. A suitable EC for Cambodia's climate condition is indirect evaporative cooling (IEC) due to the effectiveness of the air cool can be achieved without the need for additional moisture in the air. To clarify this point, this study investigated the impact of weather factors on the performance and air temperature outlet of the IEC for Cambodia's climates. Using the 2-D cross-flow model within IEC to validate condensate in a dry channel. Application in the garment factory building which has a total area is 6324 m^2 and an average cooling load of 747158.37 W. The simulation model is based on the heat and mass transfer process within IEC, as well as weather data from Phnom Penh City. The effectiveness of it is assessed using a variety of operating parameters, including ambient air inlet properties, air velocity, and wettability factors. The results revealed that the average dry-bulb temperature outlet, the COP, and wet-bulb effectiveness are 24.57℃, 219.13, and 2.79, respectively. Furthermore, the IEC system has a 0.90-year payback period when compared to the VRV system, a net saving in energy expenditures over a 30-year life cycle of $1877957.1, and reduced carbon emission is 467.62 tons per year.

Index Terms – Simulation model, Indirect evaporative cooling system, Condensation, Wettability factor, Phnom Penh.

I. INTRODUCTION

Cambodia, situated between latitudes 10° and 14° north of the equator, is a country in Southeast Asia known for its tropical monsoon climate. It experiences distinct dry and wet seasons, with the dry seasons typically lasting from November to April. The weather during this time is characterized by low humidity and little rain. On the other hand, the wet season spans from May to October, with the peak of rainfall occurring between June and September, accompanied by higher humidity levels [1]. In recent decades, there has been a significant increase in demand for cooling purposes, such as refrigeration and air conditioning, in Cambodia. It is estimated that as of 2021, there are approximately 110 thousand units in use [2]. Across developed countries in Southeast Asia, cooling accounts for around 56% of all energy usage in buildings [3]. To address the rising energy consumption associated with air conditioning systems, some factory industrial buildings in Cambodia have opted for direct evaporative cooling (DEC) systems. These systems have lower electricity consumption compared to traditional air conditioning. Reports suggest that classic vapor compression air conditioning systems use 75% more energy than DEC systems [4], [5]. DEC systems are noted for their environmental friendliness because they provide cooling without the usage of chlorofluorocarbons (CFCs) and hydrochlorofluorocarbons (HCFCs), which contribute to greenhouse gas emissions and ozone layer depletion [6]. DEC systems are frequently used as low-cost substitutes for traditional air conditioning systems, particularly in hot and dry climate zones [7].

In the field of the IEC system, a major focus is on the development of mathematical models that can solve complex configurations involving simultaneous heat and mass transfer. These models are designed to study IEC's potential as an energy-efficient cooling system and a sustainable cooling practice. Numerous researchers have examined the process of heat and mass transfer mechanisms in IEC exchangers from different perspectives [8].

To address the challenges associated with energy-intensive processes like vapor compression cycles used in conventional air conditioning systems, IEC devices are employed in conjunction with them [8]. Commonly, IEC systems utilize a plate-type exchanger by the thin plates separating parallel dry and wet channels. There are different types of IEC units, including flat plate, irregular plate, and tube types [9], [10]. The flat plate type can be further classified into three variants based on the flow pattern: parallel, counterflow, and cross-flow. Additionally, depending on the number of cooling stages, these units can be categorized as single, double, or multi-stage systems [11]–[14]. [15] proposed various approaches based on experimental methods, analytical solutions, and numerical

Nomenclatures

Q_{CC}	Cooling capacity, W	σ	Wettability factor
i	Enthalpy of moist air, kJ/kg	ω	Humidity ratio, kg/kg dry air
D_h	Hydraulic diameter, m	δ	Plate thickness, m
L	Heat transfer plate length, m	ν	Kinematic viscosity, m^2/s
L_e	Lewis factor	Subscripts	
$\dot{m}$	Mass flow rate, kg/s	x	Channel height

U	Overall heat transfer coefficient, W/m^2.K	y	Channel width
Pr	Prandtl number	z	Channel gap
Re	Reynolds number	o	Outlet
c_p	Specific heat capacity, kJ/kg ℃	i	Inlet
k	Thermal conductivity, W/m.K	int	Interface plate
V	Velocity, m/s	p	Primary air
t	Temperature, ℃	s	Secondary air
C	Cost	w	Water film
		wb	Wet-bulb
Special characters			
ε	Efficiency	cp	Capital cost
ρ	Density, kg/m^3	opt	Operation cost
Γ	Spray water density, kg/(m.s)	m	Maintenance cost

simulations to describe the IEC features of the Maisotsenko cycle (M-cycle). [16] proposed a mathematical model for analyzing heat and mass flow in different IEC exchangers using the modified Ɛ-NTU technique. The simulation revealed various unexpected features, making it possible to expect their performance accurately. The findings included the calculation of optimal operating parameters as well as a gain in efficiency as a result of the input circumstances. [14] used numerical methods to cool air to dew point temperature in the counter-flow and cross-flow of the IEC systems. To increase efficiency, various operational situations and design parameters were outlined. Additionally, the design of IEC units is crucial in expanding their application space and efficiency.

In hot and dry climates where there is no condensation in the dry channel, IEC systems are widely used. Because condensation can form in the dry channel in hot and humid regions, IEC is used in conjunction with vapor-compression coolers to pre-cool incoming air. [17] presented research on a unique cross-flow of the IEC system that utilizes condensation from the primary air as a heat recovery device. Because the counter-flow of the IEC condensation ratio is 2-15% higher than in the cross-flow IEC system, wet-bulb effectiveness is lowered by 2-7% while operating under the same conditions. [10] proposed a 2D analytical model that takes primary air condensation into account for IEC verification. According to the findings, condensation is most likely to occur at the cross-flow IEC system's primary air exit and secondary air input. [18] used a numerical model to explore non-condensation, partial-condensation, and full-condensation situations in the process of heat and mass transfer within a cross-flow of the IEC systems. The findings demonstrated that the three condensation states of a dry channel are affected by operational variables including the inlet air temperature, humidity ratio, air velocity, and wettability factor. Moreover, to design a system relevant to natural ventilation like an IEC system to provide thermal comfort in natural ventilation. [19] reported a study in which industrial electric fans (wall fan, oscillating ceiling fan, fixed ceiling fan, and desk fan) were positioned behind participants and the air velocity was altered. The results suggest that constructing an air ventilation system for a non-conditioned structure within the limit of air velocity not exceeding 3 m/s, and indoor conditions for a maximum air temperature of around 36.3℃ and relative humidity ranging from 50% to 80% for Thailand and surrounding countries. [20] reported a study in which participants filled out a questionnaire while simultaneously undergoing physical measurements to investigate thermal comfort in natural ventilation. The results reveal that the comfort temperature for Thai people in the residential building is between 25.5℃ to 30.5℃ with air velocity of 0.32 m/s to 0.74 m/s.

This study aims to investigate the performance of an indirect evaporative cooling (IEC) system in Cambodia's climate while considering its economic benefits and environmental effects. The analysis involves examining weather conditions and primary air temperature outlets using a 2-D model cross-flow. The simulation incorporates the principles of heat and mass transfer and includes non, partial, and full condensation within the IEC systems, considering various operating conditions such as ambient air inlet properties, wettability factors, and primary and secondary air velocities. The ultimate goal is to assess the system's effectiveness in achieving thermal comfort through natural ventilation. The study's findings can be used to evaluate the performance of IEC systems in Cambodia's climate.

II. SIMULATION METHODOLOGY

2.1 Description of cross-flow heat exchanger in the IEC

The IEC device is made up of thin, flat plates that serve as heat and mass exchangers and are put in a water basin, as well as a water circulation pump, water spray nozzles installed over the plate, and a supply and exhaust air fan. The heat exchangers utilize both the IEC's primary (product, supply) and secondary (working, exhaust) air. When water is sprayed from the nozzles in the heat exchanger, some of it adheres to the walls and forms a liquid film, as depicted in Figure 1. Additionally, small droplets mixed into the atmosphere within the wet channel. The IEC system uses evaporative cooling to cool the primary air in the dry channel, which is caused by a transfer of heat and mass between the water that cools and the secondary air through the wet channel. The plate temperature decreased because of the evaporative cooling effects within the wet channel, which allowed the principal air to continue to exchange heat throughout the plate without coming into touch with the water film. IEC is a widely recognized cooling and air conditioning system in various fields such as industrial, residential, markets, data centers, etc.

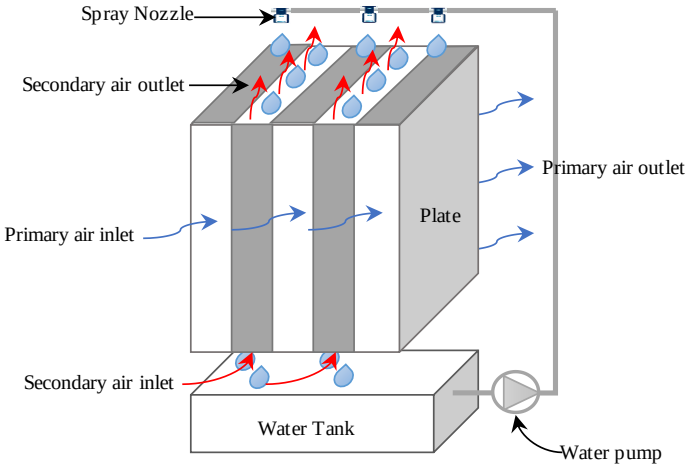


Figure 1. Scheme of the 2-D model cross-flow of the IEC

2.2 Condensation States in the heat exchanger

Non-condensation happens under less warm (or cool) weather and dry air conditions because the dew-point temperature is always lower than the plate temperature along the airflow direction. When the relative humidity of the entering air is insufficient to cause instant condensation, partial condensation can occur. When the air is sufficiently humid, the plate temperature falls below the dew-point temperature along the airflow direction, resulting in full-condensation and complete coverage of the plate surface with a water film [10] as shown in Figure 2, while the IEC system is used in Cambodia's climate, the operational state of the IEC system can be categorized as non, partial, and full-condensation.

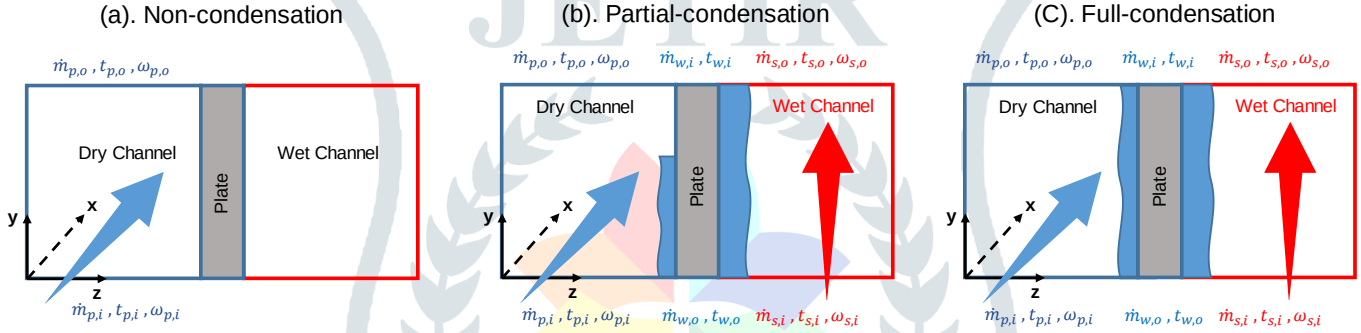


Figure 2. A schematic representation of the condensation states in the IEC's cross-flow

2.3 Mathematical 2-D model cross-flow equations

The IEC system was simulated using a mathematical model that included heat and mass balance equations in both the dry and wet channels. The model was implemented using Visual Basic for Applications (VBA). To accurately represent the IEC system's behavior, the primary and secondary air conditions were based on weather data specific to Phnom Penh City's climate. In the process of developing the mathematical model, certain assumptions were made to facilitate its implementation and ensure a practical approach. These assumptions include:

- Indirect evaporative cooling has no heat exchange to the surrounding (adiabatic system)
- The plate wall and water film are so thin, thermal resistances are insignificant, and the temperature is the same as the plate [21]
- The fluid flows are fully developed, and the fluid's thermal properties are stable
- The water is distributed evenly over the entire passage.
- The heat and mass are only transported in the direction of the fluid's flow [17]
- At the water temperature, the secondary air that comes into touch with the water film is saturated [18].

2.3.1 Primary airflow

- In the non-condensation, the mass flow rate of the primary air of the IEC can be calculated from Eq. 1 [18]:

$$\dot{m}_p = \frac{1}{2}\rho_{p,i} V_{p,i} L_z L_y \qquad \text{(Eq. 1)}$$

The IEC's overall heat and mass transfer coefficient can be calculated:

$$U = 1/\left(\frac{1}{h_p} + \frac{\delta_{wall}}{k_{wall}}\frac{1}{h_w}\right) \qquad \text{(Eq. 2)}$$

The IEC dimensionless parameter that can be determined is the number of transfer units:

$$NTU = \frac{UA}{\dot{m}_p c_{p,a}} \qquad \text{(Eq. 3)}$$

The outlet of air humidity ratio in an IEC dry channel can be stated as:

$$\omega_{p,o} = \omega_{p,i} = \text{constant} \qquad \text{(Eq. 4)}$$

The primary air temperature outlet of the IEC assumed:

$$t_{p,o} = t_{p,i} = \text{constant} \quad \text{(Eq. 5)}$$

- In partial-condensation or full-condensation, the humidity ratio of air outlet in a dry channel of the IEC can be calculated from Eq. 7 [18]:

$$\frac{\partial \omega_{p,i}}{\partial x} = NTU \frac{\sigma}{L_e L_x}(\omega_{\text{int}} - \omega_{p,i}) \quad \text{(Eq. 6)}$$

$$\frac{\partial \omega_{p,i}}{\partial x} = NTU \frac{\sigma}{L_e L_x}(\omega_{\text{int}} - \omega_{p,i}) \quad \text{(Eq. 7)}$$

The primary air temperature outlet of the IEC can be calculated as:

$$\frac{\partial t_{p,i}}{\partial x} = \frac{1}{L_x}(NTU(t_{w,i} - t_{p,i})\sigma + NTU \frac{\sigma c_{p,v}}{L_e c_{p,a}}(\omega_{\text{int}} - \omega_{p,i})(t_{w,i} - t_{p,i})) \quad \text{(Eq. 8)}$$

$$t_{p,o} = t_{p,i} + (\frac{\partial t_{p,i}}{\partial x})dx \quad \text{(Eq. 9)}$$

2.3.2 Coefficients of heat and mass Transfer

The mass transfer coefficient could be obtained by the following:

$$h_m = \frac{h}{c_p L_e} \quad \text{(Eq. 10)}$$

The coefficient of convective heat transfer in the IEC's dry channel can be computed using Eq. 11 [22]:

$$h_p = \frac{0.0238(V_{p,i}/\nu_{p,i})^{0.8} pr_{p,i}^{0.3} k_{p,i}}{D_h^{0.2}} \quad \text{(Eq. 11)}$$

The coefficient of convective heat transfer in the IEC's wet channel can be computed using Eq. 12 [23]:

$$h_s = \frac{36.31(\rho_{s,i} V_{s,i})^{0.68}}{(L_y / D_h)^{0.08}} \quad \text{(Eq. 12)}$$

The coefficient of convective heat transfers the water film can be calculated from:

$$h_w = 1.88 \frac{k_w}{\delta_w} \quad \text{(Eq. 13)}$$

In the IEC unit, the airflow could be considered a laminar flow, and for a laminar flow across a vertical plate, the film thickness, flow rate per length, and hydraulic diameter could be determined using the formulas below [10], [24]:

$$\delta_w = \left(\frac{3\nu_w \Gamma_w}{\rho_w g}\right)^{1/3} \quad \text{(Eq. 14)}$$

$$\Gamma_w = \frac{m_w}{(n+1)L_y} \quad \text{(Eq. 15)}$$

$$D_h = \frac{2L_x L_y}{L_x + L_y} \quad \text{(Eq. 16)}$$

In the air temperature range 0℃ to 100℃, Eq. 17 might be used to compute the humidity ratio of saturated air at the plate surface temperature [25]:

$$\omega_{\text{int}} = 0.622 \frac{P_{ws}}{P - P_{ws}} \quad \text{(Eq. 17)}$$

$$P_{ws} = P_0 \times 10^{t_w/(a_1 + a_2 t_w + a_3 t_w^2)} \quad \text{(Eq. 18)}$$

Where $P_0 = 610.7Pa$, $a_1 = 31.6639$, $a_2 = 0.131305$, and $a_3 = 2.63247 \times 10^{-5}$.

In VBA simulation, the boundary conditions for the above-mentioned equation are primary air temperature inlet $t_{p,o}(x=0) = t_{p,i}$, primary air humidity ratio inlet $\omega_{p,o}(x=0) = \omega_{p,i}$, secondary air temperature inlet $t_{s,o}(y=0) = t_{s,i}$, and secondary humidity ratio inlet $\omega_{s,o}(y=0) = \omega_{s,i}$.

2.3.3 Evaluations of performance

The IEC's wet-bulb effectiveness can be determined as follows:

$$\varepsilon_{wb} = \frac{t_{p,i} - t_{p,o}}{t_{p,i} - t_{wb,i}} \quad \text{(Eq. 19)}$$

The total cooling capacity in the IEC is calculated as follows:

$$Q_{CC} = M_p(i_{p,i} - i_{p,o}) \quad \text{(Eq. 20)}$$

The IEC's coefficient of performance (COP) is expressed as follows:

$$COP = \frac{Q_{CC}}{P_{fan} + P_{pump}} \quad \text{(Eq. 21)}$$

The power consumption of the IEC's fan and pump can be stated as:

$$P_{fan} = \frac{\Delta p_p \dot{V}_p + \Delta p_s \dot{V}_s}{\eta_{fan}} \quad \text{(Eq. 22)}$$

$$P_{pump} = \frac{m_w H_{pump} g}{\eta_{pump}} \quad \text{(Eq. 23)}$$

The friction pressure loss is computed as follows:

$$\Delta P = f \frac{\rho V^2 L}{2 D_h} \quad \text{(Eq. 24)}$$

The fluid friction resistance factor for laminar flow in a rectangular channel can be computed as follows:

$$f = \frac{96}{Re} \quad \text{(Eq. 25)}$$

2.3.4 Simulation and Input Parameters

The equations were solved using the finite difference method and a partial differential equation. The VBA software was used to solve the given models and equations. First, the IEC structural parameters and operational parameters were entered. The heat and mass transfer coefficients at the interface were then computed. The equivalent moisture content of the water sheet was then estimated by assuming the plate surface temperature. Finally, the surface temperature was measured and compared to the assumed temperature of the plate surface. Table 1 lists the IEC structural parameters, and Figure 3 depicts weather data from Phnom Penh City.

Table 1. Typical operating and geometric parameters of the IEC

Parameter	Value	Units
Channel length	600	mm
Channel width	600	mm
Channel gap	5	mm
Plate thickness	0.15	mm
Channel pair	240	-
Mass flow of the spay water	0.768	kg/s
Water film temperature	22	℃
The velocity of primary air	2.5	m/s
The velocity of secondary air	2.5	m/s
Material	aluminum	-

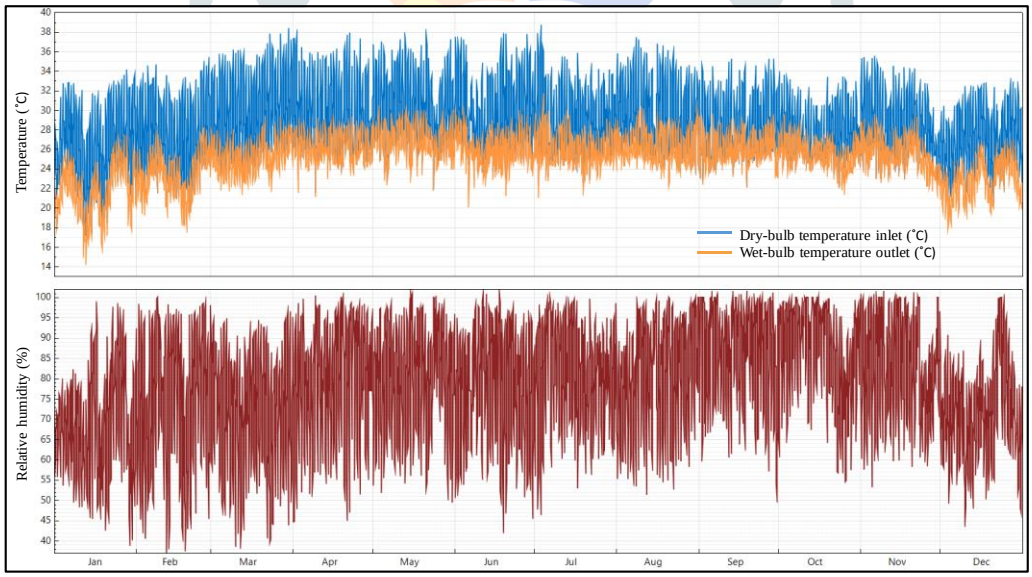


Figure 3. The weather data in Phnom Penh City

2.3 Economic benefit of the factory building

The cooling load of a factory building was simulated by EnergyPlus. The building was designed to simulate a typical garment factory and was based on a real garment factory in Phnom Penh, as shown in Figure 4. The building is a single-space structure, measuring 93 m in length, 68 m in width, 9 m in height, and with a roof slope of 5.14 m, for a total area of 6324 m^2. For the fenestrations, there are 34 windows and 6 doors in total. The outside walls consist of 8 windows, and 3 doors on the south and north whereas on the east and the west, there are 9 windows for each side no door. The roof of the building is assumed to be fully made of zinc (Galvanized Steel).



Figure 4. A garment factory in Phnom Penh city

To assess the cooling load of the simulated building, the investigation focused on the hours of 7:00 am to 11:00 am and 13:00 pm to 17:00 pm throughout the year. The occupancy density of the building was considered to be 360 people. The cooling setpoint was set at 25℃, while the lighting intensity was 16 W/m^2, and the plug and process load were 48 W/m^2. The building operated on 240 working days in 2023. It is important to note that this building is a model and does not physically exist.

According to the modeling results, the average cooling load is 747158.37 W, with a load per area of 118.15 W/m^2. The airflow rate required for cooling was estimated to be 55.286 m3/s. Regarding the electricity cost, according to the consolidated report for 2022 issued by Electricité Du Cambodge [26], the electricity price for industrial consumers in Cambodia is $0.137 per kWh for low voltage (LV) types. The price is applicable for the simulated building's electrical consumption. For water consumption, the price from Phnom Penh Water Supply Authority [27] is reported to be $0.35 per m^3.

2.4.1 IEC system relative to the VRV system

The payback period of the IEC system in comparison to the VRV system can be determined using Eq. 26 [28]:

$$PP_{IEC} = \frac{C_{cp,vrv} - C_{cp,iec}}{(C_{opt,vrv} - C_{opt,iec}) + (C_{m,vrv} - C_{m,iec})} \quad \text{(Eq. 26)}$$

The maintenance cost of both the IEC system and the VRV system was calculated to be 1.5% of their respective capital costs [29].

Considering the 30-year life cycle of both the IEC system and the VRV system [30], the net savings in energy bills by employing the IEC system in Cambodia will be determined using the following Eq. 27:

$$C_{net,bill,sav} = (30 - PP_{IEC})\{(C_{opt,vrv} - C_{opt,iec}) + (C_{m,vrv} - C_{m,iec})\} \quad \text{(Eq. 27)}$$

The annual electricity power savings achieved by the implementation of the IEC system compared to the VRV system. These savings are measured in terms of kilowatt-hours (kWh) per year. By utilizing the equation derived from the reference [28], it is possible to convert these electricity savings into carbon emissions reduction:

$$Em_{co2} = \frac{f_{c,c} \times En_a}{1000} \quad \text{(Eq. 28)}$$

Where,

$f_{c,c}$: Carbon conversion factor to grid power, 0.6257 kg CO_2 emission per kWh power [31];
En_a: Annual electricity power savings, measured in kWh.

III. MODEL VALIDATION

The 2-D cross-flow model of an IEC system was validated using experimental results from the published citation. In the verification process, all operating conditions were kept the same as those given in references. The dry-bulb temperature and humidity ratio outlet from the dry channel was observed. Firstly, the comparison was made with the results obtained by [10], who used a cross-flow type of the IEC system with a channel length of 400.0 mm, channel width of 400.0 mm, plate thickness of 0.15 mm, and channel gap of 5.0 mm. The primary air velocity was 2.50 m/s, the relative humidity was 70%, and the primary air inlet temperature ranged from 28.0℃ to 38.0℃ at 2.0℃ intervals. Figure 5 depicts the compression results from the two models. In the dry-bulb temperature outlet, the largest difference between the models was 0.81%, while the humidity ratio outlet had a difference of 7.69%.

Secondly, the comparison was made with the results obtained by [32], who used the same geometry and parameter operating condition but increased the relative humidity inlet to 90%. The primary air temperature inlet ranged from 28.0℃ to 38.0℃ at 2.0℃ intervals. Figure 5 depicts the results of the comparison between the two models. In the dry-bulb temperature outlet, the maximum difference between the models was 3.38%, and in the humidity ratio outlet, it was 7.76%.

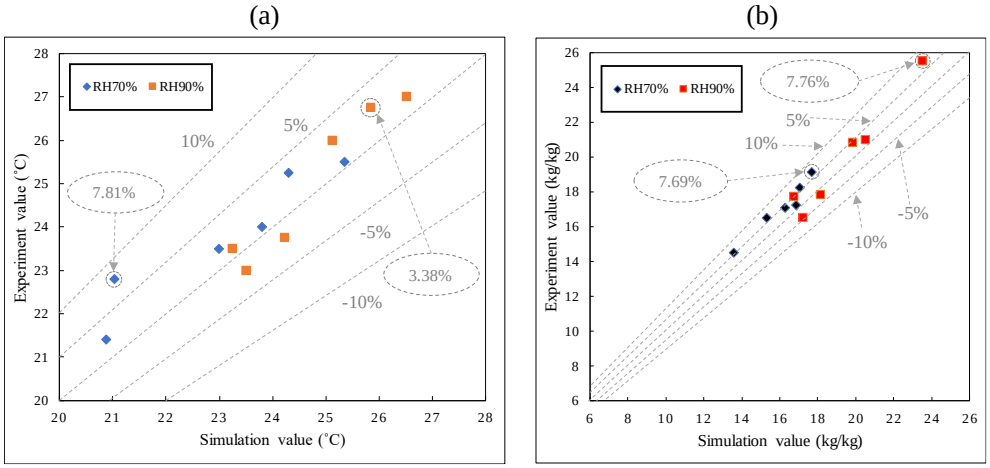


Figure 5. Comparison of the simulation results and experiment results: (a) The dry-bulb temperature outlet; (b) The humidity ratio outlet from Ref [10], [32]

IV. RESULTS AND DISCUSSION

The simulations conducted in this study aimed to examine the influence of the primary air temperature and relative humidity inlet on the performance of the indirect evaporative cooling (IEC) system. Figure 3 illustrates the weather data for operation, considering an air velocity of 2.50 m/s. The key parameters investigated were the dry-bulb temperature outlet through the dry channel, wet-bulb effectiveness ($\mathcal{E}_{wb}$), and the coefficient of performance (COP). Additionally, the study evaluated the economic benefits of the IEC system compared to a traditional vapor-compression cooling system and its environmental effects.

4.1 Influence of primary air temperature and relative humidity

Varying the inlet primary air temperature and relative humidity based on the weather data in Phnom Penh City over a year as shown in Figure 3 while the various parameters remain unchanged, the simulation was carried out using the above-established IEC model and the results are presented in Figure 6, displays the variation for supply air temperature and relative humidity in the three condensation state (non, partial, and full-condensation), the lower supply air temperature can be observed, particularly during March, April, May, June, July, August, September, October, and November when the weather is typically hot and humid. This is because the high temperature at the inlet enhances heat transfer between two channels, resulting in improved cooling capacity, this observation aligns with the results obtained by [14]. On the other hand, during some days in January, February, and December when the weather is cool (or less warm) and dry, the IEC system does not need to operate, and the outlet temperature will be the same as the ambient air temperature, and it's increasing while the ambient air less warm and dry.

The yearly averages for supply air temperature, relative humidity, and temperature difference between supply air temperature and ambient air temperature were 24.57℃ (±2.32℃ SD), 86.74% (±12.21% SD), and 3.63℃ (±3.23℃ SD), respectively. According to the experience of weather in Cambodia [1] the IEC unit, it's can provide more thermal comfort in condition spaces such as industrial, residential, and data centers based on the [19], [20] who presented the thermal comfort had weathered the same Cambodia. Furthermore, this system does not additional moisture into the supply air temperature because the air passing through the system does not come into contact with water spray in the wet channel. The supply air temperature in thermal comfort is 99.95% and it does not thermal comfort is 0.05% for the thermal comfort in natural ventilation from the references.

To explore the hourly day variation for the dry-bulb temperature outlet of the IEC system over a year, Figure 7 provides a heat map detailing all the dry-bulb temperature outlets.

Accordingly, Figure 8 illustrates the variation in power consumption and cooling capacity of the IEC system for an air velocity of 2.50 m/s. When the ambient air is cool (or less warm) and dry, the system operates in non-condensation mode, requiring only one fan to supply air into space. It consumes a power of 14.91 W but does not provide any cooling capacity (0.00 W). However, when the weather is hot and humid, the system operates in either partial-condensation or full-condensation mode. In these modes, two fans (an exhaust air fan and a supply air fan) and one pump (the wet channel water spraying pump) are active. The total power consumption increases to 45.55 W, and the system achieves a maximum cooling capacity of 60741.54 W.

Consequently, the annual average power consumption and cooling capacity are determined to be 39.46 W and 9838.36 W, respectively.

Referring to Figure 9 displays the variation in wet-bulb effectiveness and coefficient of performance (COP). the wet-bulb effectiveness decreases as the inlet air becomes cool (or less warm) and dry. Conversely, it increases with hot and humid inlet air. The highest wet-bulb effectiveness value is observed when the air approaches its saturation point. The COP of the IEC system is influenced by numerous parameters such as the temperature differential between the primary air temperature inlet and outlet, humidity ratio, air velocity, mass flow rate, and geometric system [18]. The COP rises as the temperature rises, due to a higher temperature difference between the inlet air and the water spray induced by hotter inlet air. Therefore the transfer of heat between both channels can be enhanced by rising temperatures in the inlet air, which is consistent with the results obtained by [14], [18]. The annual average of the wet-bulb effectiveness and COP were 2.79, and 219.13, respectively.

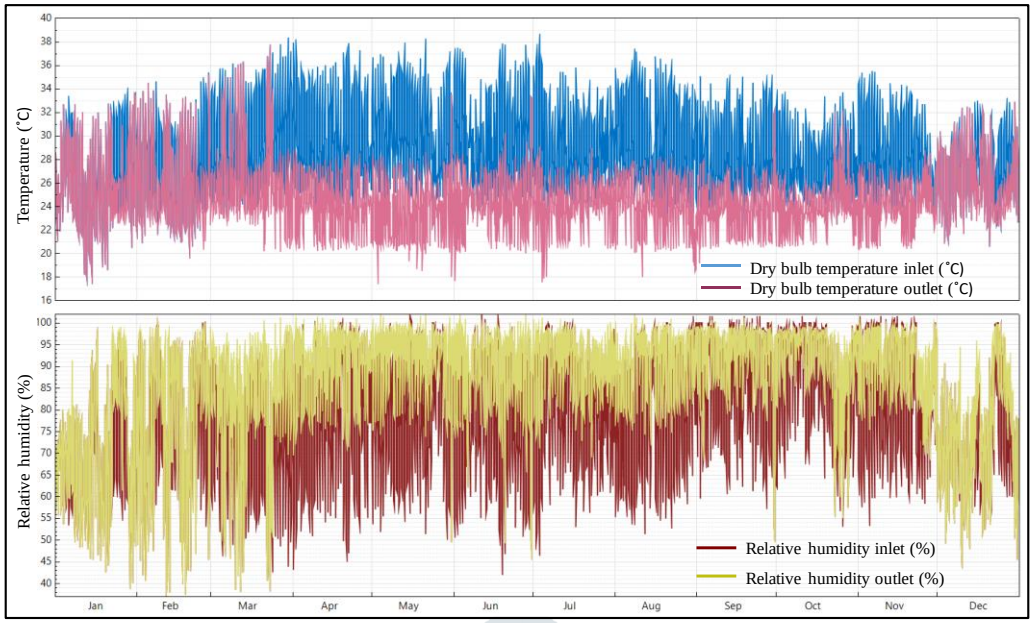


Figure 6. Dry-bulb temperature and Relative humidity inlet and outlet of the IEC

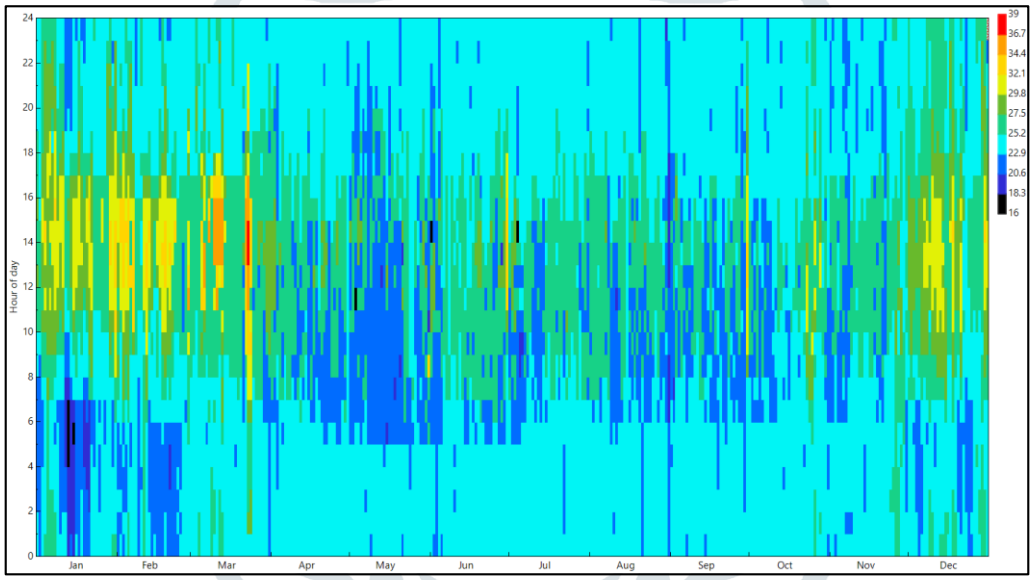


Figure 7. Heat map for the dry-bulb temperature outlet of the IEC

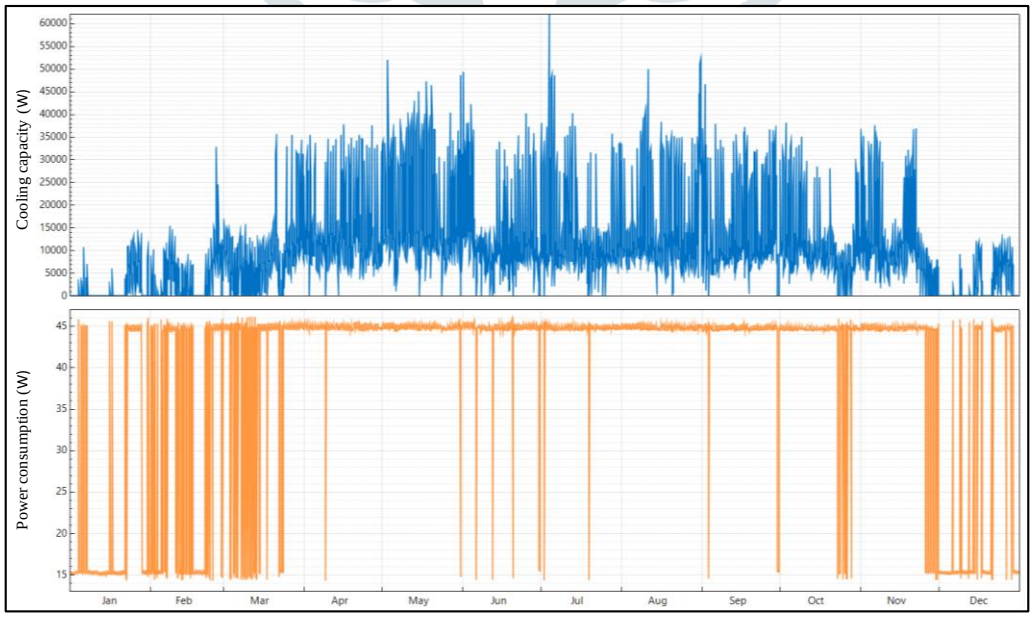


Figure 8. Power consumption and cooling capacity of the IEC

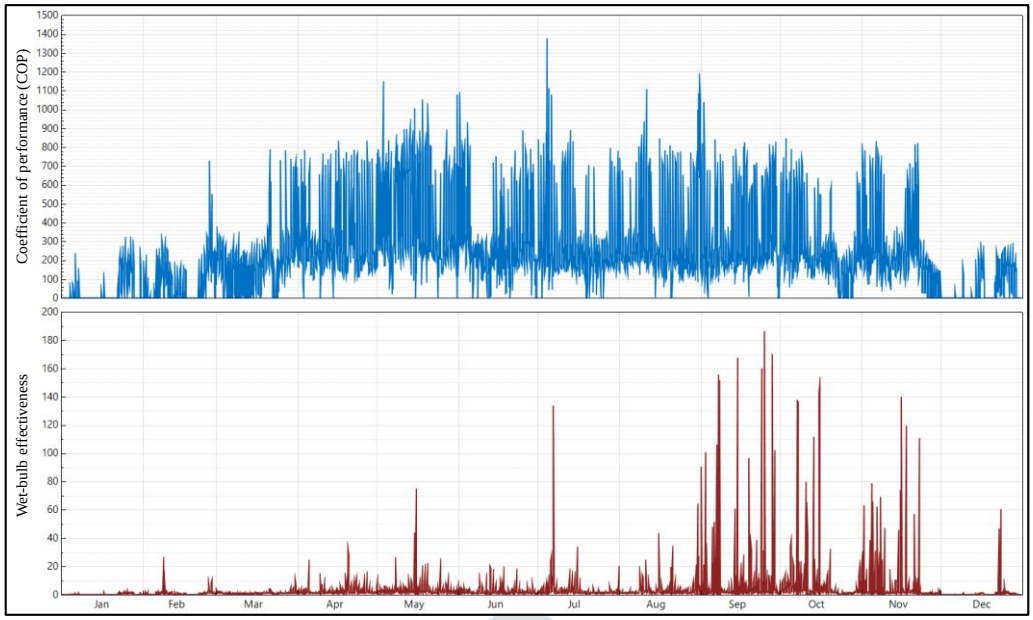


Figure 9. Coefficient of performance (COP) and Wet-bulb effectiveness of the IEC

4.2 Evaluation of the economic benefit of the IEC system relative to the VRV system

According to EnergyPlus simulations, the average cooling load of a garment factory building is 747158.37 W (or 2556028.8 Btu/h), with a load per area of 118.15 W/m^2. To model a VRV system for this building, we assume RXQ54AMYM for the outdoor unit, FXMQ80PVE, and FXMQ250MAVE for the indoor unit, with 5, 5, and 25 units, respectively, to provide a cooling capacity more than the cooling capacity in this building. The total capital cost for this VRV system is estimated to be $189245, with an operating cost of $70244.83 per annum, and a maintenance cost of $2838.68 per annum as shown in Table 2. Alternatively, an IEC system can be used in this building, with an average temperature setting of 25℃ from 7:00 am to 11:00 am and 13:00 pm to 17:00 pm, and an average cooling capacity of 12942 W from simulation results as shown in Figure 10. For this, we would need 58 indoor units of the IEC system, with an assumption capital cost of $131120.6, operating cost of $6580.65 per annum, and maintenance cost of $1966.81 per annum as shown in Table 3.

According to the results of the technical parameters of both the systems, the energy saving, capital cost saving, and operation cost saving are 91.18% per annum, $58124.4, and $ 64536.05 per annum as compared to the VRV system. Based on the calculation, the payback period for the IEC system vs the VRV system for this garment factory building is 0.9 years. Furthermore, the net savings in energy expenses for both systems during a 30-year life cycle are $1877957.1, as shown in Table 4.

Table 2. Technical parameters of the VRV system

Model	Cooling capacity (Btu/h)	Power consumption (kWh)	Quantity (pcs)	Unit price ($)	Cost ($)	Operation cost ($)	Maintenance cost ($)
RXQ54AMYM	512000	45.9	5	19929	99645	60367.68	1494.68
FXMQ250MAVE	95500	01.467	25	3390	84750	9633.84	1271.25
FXMQ80PVE	30700	0.185	5	970	4850	24.31	72.75

Table 3. Technical parameters of the IEC system

Description	Unit	Value
IEC	pcs	58
Supply air flow rate per unit	m^3/h	3240
Supply air temperature per unit	℃	25
Cooling capacity per unit	W (or Btu/h)	12942 (or 44158.104
Power consumption per unit	W	406
Energy efficiency per unit		31.9
Total capital cost	$	131120.6
Total operation cost per year	$	6580.65
Total maintenance cost per year	$	1966.81

Table 4. The economic advantage of the IEC system over the VRV system

City	Phnom Penh
Energy saving per year, %	91.18
Capital cost saving, $	58124.4
Operational cost saving per year, $	64536.05
Payback period, year	0.9
Net energy bill saving over the 30-life cycle, $	1877957.1

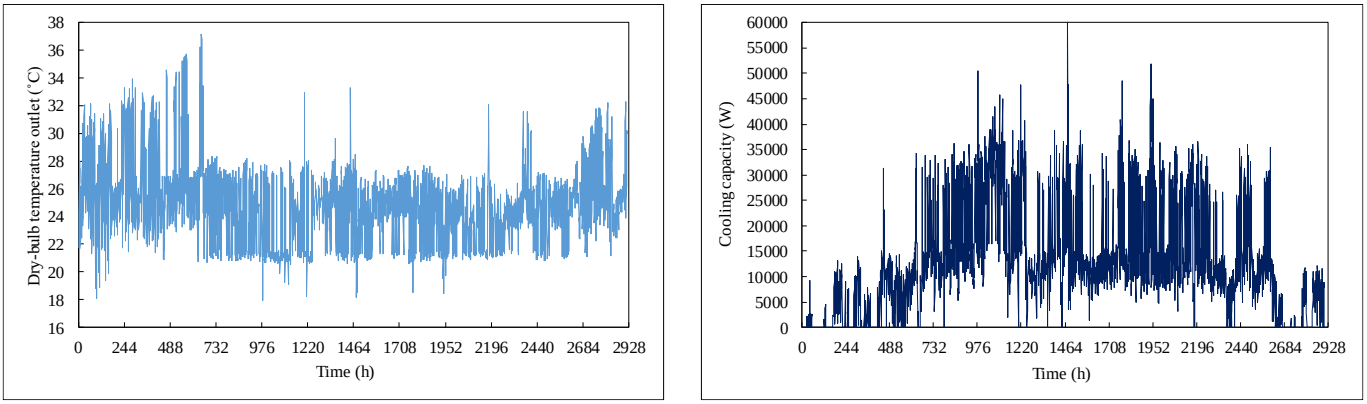


Figure 10. Dry-bulb temperature outlet and Cooling capacity of the IEC from 7:00 am to 11:00 am and 13:00 pm to 17:00 pm

4.3 Environmental effect

The calculated results indicate that the garment factory building space requires 6324 m^2, and it can be effectively cooled using an indirect evaporative cooling unit with a range of 750636 W. The cooling unit operates from 7:00 am to 11:00 am and 13:00 pm to 17:00 pm, resulting in an annual reduction of 467.62 tons of CO_2 emissions.

In addition to air cooling capabilities, the use of the IEC system offers significant environmental benefits. One notable advantage is the opportunity to eliminate the reliance on CFCs (chlorofluorocarbons) and HCHCs (hydrochlorofluorocarbons) as refrigerants. These substances have been scientifically proven to contribute directly to the ozone layer depletion and subsequent global warming.

V. Conclusion

The 2-D simulation cross-flow model is derived from heat and mass transfer within the IEC to analyze the performance of the IEC system for Cambodia's climate. The simulation results of this study demonstrate that the IEC system is suitable for Cambodia's climate, considering the outlet temperature, performance, economic benefit of the IEC system, and environmental effect. The performance and other relevant to support the conclusion in this study are the following;

- The primary air temperature outlet decreases when the weather is hot and humid or cool and dry, and increases when the weather is less warm and dry. The yearly average outlet temperature of primary air and relative humidity are 24.57℃ (±2.32℃ SD), and 86.74% (±12.21% SD), respectively. The supply air temperature in thermal comfort is 99.95% and 0.05% uncomfortable.
- The wet-bulb effectiveness is highest when the inlet temperature approaches the saturation point and the COP increase while the inlet temperature increase. The average wet-bulb effectiveness and coefficient of performance (COP) over the year are 2.79 and 219.13, respectively.
- For both systems anticipated in the garment factory building in Phnom Penh City, the payback period for the IEC system is 0.90 years and the net savings in energy costs for a 30-year life cycle is $1877957.1.
- For the 750636 W rating indirect evaporative cooling (IEC) system, its annual carbon emission could be reduced by 467.62 tons compared to the VRV system.

VI. Acknowledgment

The authors gratefully acknowledge the support from the Thermal Laboratory members at the Institute of Technology of Cambodia, and the scholarship from Svay Rieng University under Higher Education Improvement Project (HEIP: Grant No. 6221-KH).

References

[1] G. McSweeney, C.; New, M.; Lizcano, "UNDP Climate Change Country Profiles Cambodia," Available online, pp. 1–27, 2013, [Online]. Available: http://ncsp.undp.org/sites/default/files/Cambodia.lowres.report.pdf

[2] Leander von Kameke, "Air conditioning demand in Cambodia 2012-2021," 2023. [Online]. Available: https://www.statista.com/statistics/909991/cambodia-ac-demand-units/#statisticContainer

[3] A. R. Katili, R. Boukhanouf, and R. Wilson, "Space Cooling in Buildings in Hot and Humid Climates—A Review of the Effect of Humidity on the Applicability of Existing Cooling Techniques," Proc. 14th Int. Conf. Sustain. Energy Technol., no. August, pp. 25–27, 2015, doi: 10.13140/RG.2.1.3011.5287.

[4] Y. Cerci, "A new ideal evaporative freezing cycle," Int. J. Heat Mass Transf., vol. 46, no. 16, pp. 2967–2974, 2003, doi: 10.1016/S0017-9310(03)00072-3.

[5] D. Bishoyi and K. Sudhakar, "Experimental performance of a direct evaporative cooler in composite climate of India," Energy Build., vol. 153, pp. 190–200, 2017, doi: 10.1016/j.enbuild.2017.08.014.

[6] I. Kovačević and M. Sourbron, "The numerical model for direct evaporative cooler," Appl. Therm. Eng., vol. 113, no. November, pp. 8–19, 2017, doi: 10.1016/j.applthermaleng.2016.11.025.

[7] S. A. Nada, H. F. Elattar, M. A. Mahoud, and A. Fouda, "Performance enhancement and heat and mass transfer characteristics of direct evaporative building free cooling using corrugated cellulose papers," Energy, vol. 211, p. 118678, 2020, doi: 10.1016/j.energy.2020.118678.

[8] G. Zhu, T. T. Chow, and C. K. Lee, "Performance analysis of counter-flow regenerative heat and mass exchanger for indirect evaporative cooling based on data-driven model," Energy Build., vol. 155, pp. 503–512, 2017, doi: 10.1016/j.enbuild.2017.09.053.

[9] D. Pandelidis, A. Cichoń, A. Pacak, S. Anisimov, and P. Drąg, "Counter-flow indirect evaporative cooler for heat recovery in the temperate climate," Energy, vol. 165, pp. 877–894, 2018, doi: 10.1016/j.energy.2018.09.123.

[10] B. Zheng, C. Guo, T. Chen, Q. Shi, J. Lv, and Y. You, "Development of an experimental validated model of cross-flow

indirect evaporative cooler with condensation," Appl. Energy, vol. 252, no. 26, p. 113438, 2019, doi: 10.1016/j.apenergy.2019.113438.
[11] X. Cui, X. Yang, Q. Kong, X. Meng, and L. Jin, "Performance evaluation and comparison of multistage indirect evaporative cooling systems in two operation modes," Int. J. Energy Res., vol. 44, no. 12, pp. 9298–9308, 2020, doi: 10.1002/er.4803.
[12] M. H. Mahmood, M. Sultan, T. Miyazaki, S. Koyama, and V. S. Maisotsenko, "Overview of the Maisotsenko cycle – A way towards dew point evaporative cooling," Renew. Sustain. Energy Rev., vol. 66, pp. 537–555, 2016, doi: 10.1016/j.rser.2016.08.022.
[13] A. Sohani and H. Sayyaadi, "Thermal comfort based resources consumption and economic analysis of a two-stage direct-indirect evaporative cooler with diverse water to electricity tariff conditions," Energy Convers. Manag., vol. 172, no. June, pp. 248–264, 2018, doi: 10.1016/j.enconman.2018.07.008.
[14] C. Zhan, X. Zhao, S. Smith, and S. B. Riffat, "Numerical study of a M-cycle cross-flow heat exchanger for indirect evaporative cooling," Build. Environ., vol. 46, no. 3, pp. 657–668, 2011, doi: 10.1016/j.buildenv.2010.09.011.
[15] H. Sadighi Dizaji, E. J. Hu, and L. Chen, "A comprehensive review of the Maisotsenko-cycle based air conditioning systems," Energy, vol. 156, pp. 725–749, 2018, doi: 10.1016/j.energy.2018.05.086.
[16] S. Anisimov, D. Pandelidis, and J. Danielewicz, "Numerical analysis of selected evaporative exchangers with the Maisotsenko cycle," Energy Convers. Manag., vol. 88, pp. 426–441, 2014, doi: 10.1016/j.enconman.2014.08.055.
[17] Y. Min, Y. Chen, and H. Yang, "Numerical study on indirect evaporative coolers considering condensation: A thorough comparison between cross flow and counter flow," Int. J. Heat Mass Transf., vol. 131, pp. 472–486, 2019, doi: 10.1016/j.ijheatmasstransfer.2018.11.082.
[18] A. Adam, D. Han, W. He, M. Amidpour, and H. Zhong, "Numerical investigation of the heat and mass transfer process within a cross-flow indirect evaporative cooling system for hot and humid climates," J. Build. Eng., vol. 45, no. October 2021, p. 103499, 2022, doi: 10.1016/j.jobe.2021.103499.
[19] J. Khedari, N. Yamtraipat, N. Pratintong, and J. Hirunlabh, "Thailand ventilation comfort chart," 2000.
[20] P. Rangsiraksa, "Thermal comfort in Bangkok residential buildings ," no. September, pp. 6–8, 2006.
[21] L. Zaheed and R. J. J. Jachuck, "Review of polymer compact heat exchangers, with special emphasis on a polymer film unit," Appl. Therm. Eng., vol. 24, no. 16, pp. 2323–2358, 2004, doi: 10.1016/j.applthermaleng.2004.03.018.
[22] S. De Antonellis, C. M. Joppolo, P. Liberati, S. Milani, and F. Romano, "Modeling and experimental study of an indirect evaporative cooler," Energy Build., vol. 142, pp. 147–157, 2017, doi: 10.1016/j.enbuild.2017.02.057.
[23] Y. Wan, A. Soh, Y. Shao, X. Cui, Y. Tang, and K. J. Chua, "Numerical study and correlations for heat and mass transfer coefficients in indirect evaporative coolers with condensation based on orthogonal test and CFD approach," Int. J. Heat Mass Transf., vol. 153, p. 119580, 2020, doi: 10.1016/j.ijheatmasstransfer.2020.119580.
[24] P. J. Erens and A. A. Dreyer, "Modelling of indirect evaporative air coolers," Int. J. Heat Mass Transf., vol. 36, no. 1, pp. 17–26, 1993, doi: 10.1016/0017-9310(93)80062-Y.
[25] W. Zalewski and P. A. Gryglaszewski, "Mathematical model of heat and mass transfer processes in evaporative fluid coolers," Chem. Eng. Process. Process Intensif., vol. 36, no. 4, pp. 271–280, 1997, doi: 10.1016/S0255-2701(97)00006-8.
[26] EDC, "Decision tariff 2022 EDC 6 provinces," 2022. [Online]. Available: https://www.eac.gov.kh/document/tariffdecidelist
[27] PPWSA, "Phnom Penh Water Supply Authority (PPWSA)," 2019. [Online]. Available: https://opendevelopmentcambodia.net/km/profiles/access-to-public-service/ppwsa-water-consumption-tariff/
[28] Z. Duan, "Investigation of a novel dew point indirect evaporative air conditioning system for buildings," Phd Diss., no. September, p. 189, 2011, [Online]. Available: http://etheses.nottingham.ac.uk/12200/
[29] T. Supervisor and A. A. Sonin, "Evaporative Air Conditioner for Automotive Application," Mech. Eng., 1994.
[30] J. D. Palmer, "Evaporative cooling design guidelines manual for New Mexico schools, and commercial buildings," NRG Eng., vol. 2626, pp. 1–99, 2002.
[31] M. of Environment and Cambodia, "Grid Emission Factor of the Phnom Penh Electricity Grid Updated as of March 2011," Phnom Penh, 2011.
[32] C. Guo, Q. Liu, B. Zheng, Y. You, and Y. Li, "Development of model based on condensation area ratio and e ff ect on heat transfer capacity of indirect evaporative cooling," Appl. Therm. Eng., vol. 164, no. September 2019, p. 114557, 2020, doi: 10.1016/j.applthermaleng.2019.114557.